CrystEngComm

Accepted Manuscript

This article can be cited before page numbers have been issued, to do this please use: M. Alonso-Orts, A. Sanchez, I. Lopez, E. Nogales, J. Piqueras and B. Mendez, *CrystEngComm*, 2017, DOI: 10.1039/C7CE01311F.

ROYAL SOCIETY OF CHEMISTRY

rsc.li/crystengcomm

View Article Online
DOI: 10.1039/C7CE01311F

Crystal Engineering Communications

ARTICLE

3D and 2D growth of SnO_2 nanostructures on Ga_2O_3 nanowires: Synthesis and structural characterization

Received 00th July 20xx,
Accepted 00th July 20xx

DOI: 10.1039/x0xx00000x

www.rsc.org/

M. Alonso-Orts,[a] A. M. Sánchez,[b] I. López,[a,c] E. Nogales,[a] J. Piqueras[a] and B. Méndez[a]

In this work, a simple thermal evaporation method has been used to obtain a variety of Ga_2O_3/SnO_2 nano-assemblies with different shape and dimensionality, which may affect their physical properties, especially those influenced by surface properties. The obtained nanostructures have been characterized by electron microscopy related techniques in order to understand the growth mechanisms. By using both metallic gallium and tin oxide powders precursors, Ga_2O_3 nanowires (straight or branched) decorated with SnO_2 nanoparticles or SnO_2 quasi-two dimensional plates have been produced after dynamic thermal annealing for 2.5, 8.0 and 15.0 hours. For shorter treatments, Sn segregation at the Ga_2O_3 nanowires surface or defect planes have been observed by high resolution TEM, which suggests that they could act as nucleation sites for further growing of SnO_2. On the other hand, longer treatments promote the formation of Ga doped SnO_2 belts, from which SnO_2 nanowires eventually emerge. High-resolution TEM imaging and microanalysis reveal that Ga accumulation at (200) SnO_2 planes could stabilize some non-stoichiometric or intermediate tin oxide phases, such as Sn_2O_3, at local areas in the belts. The presence of non-stoichiometric tin oxide is relevant in applications, since surface states affect the physical-chemical behavior of tin oxide.

Introduction

Transparent conductive oxides (TCO), which merge optical transparency and electrical conductivity, find most of their applications in optoelectronic devices. A key advantage of TCO nanostructures is their surface properties. In particular, chemical sensors and ultraviolet (UV) solar-blind photodetectors based on tin oxide and gallium oxide thin films and/or nanomaterials have been already achieved[1-3]. The morphology of TCO nanostructures plays a key role in tailoring their physical properties and functionalities. As an example, branched nanostructures have been found to improve the performance in lasers and solar cells devices, due to their high surface-volume ratio and the available efficient pathways for carrier transport[4,5]. Moreover, engineering shape at the nanoscale that include 1D, 2D or 3D oxides entities would be a further step in the design of novel nanostructures to upgrade their functionalities. This research is still at the initial stage and one of the challenges to face is the control of the growth process. Tin oxide is a suitable material for this goal. Previous works on the growth of SnO_2 nanowires, nanobrushes, microcubes or dodecahedral crystals have been reported[6-8]. In addition, the number of works on 2D oxides is steeply increasing following the trail of graphene, since many of them exhibit weak bonds within the cell unit and exfoliate easily[9-10]. Although there are several synthesis methodologies, the thermal evaporation using a metal catalyst, is a successful route to fabricate a plethora of morphologies in semiconducting oxide nanostructures, from single nanowires or nanorods to hierarchical nanostructures [11,12]. In previous works, we demonstrated the growth of single and complex oxide nanostructures using thermal evaporation by a catalyst free vapor-solid (VS) process, and under a dynamic atmosphere[13,14]. The precursors, temperature, duration of the thermal treatment and gas flow play a key role in the final morphology and physical properties of the nanostructures. The thermal evaporation method also produces doped nanomaterials by adding the appropriate chemicals to the precursors[15,16]. The incorporation of impurities would produce not only doped nanostructures but also mixed oxides complex nanostructures. The influence of Sn doping on the Ga_2O_3 and Cr doping on SnO_2 nanostructures morphology has been recently reported[13,16]. Furthermore, the addition of a certain amount of Sn and/or Cr into the precursor for Ga_2O_3 nanowires influences the growth and orientation of the nanowires and leads to mixed SnO_2/Ga_2O_3 nano-heterojunctions such as SnO_2/Ga_2O_3 crossing wires or Ga_2O_3 nanowires decorated with SnO_2 particles[18]. These architectures provide local heterojunctions that could be of interest in device applications. The mechanisms involved in the VS growth of nanostructures are complex and still not well understood. In the case of nanowires, the required anisotropy to promote the growth in one direction is provided by thermodynamic considerations of minimum surface energy. However, the achievement of nanomaterials

[a] Departamento de Física de Materiales, Facultad de Ciencias Físicas, Universidad Complutense de Madrid, 28040-Madrid, Spain.
[b] Department of Physics, University of Warwick, Coventry, CV4 7AL, United Kingdom.
[c] Istituto Nazionale di Ottica (INO), via Carrara 1, 50019 Sesto Fiorentino FI, Italy.
See DOI: 10.1039/x0xx00000x

View Article Online
DOI: 10.1039/C7CE01311F

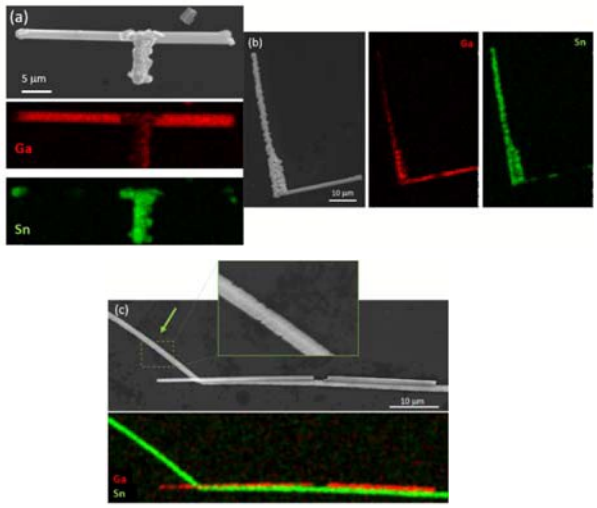

Fig. 1 SEM images and their corresponding Sn and Ga elemental mappings of structures obtained after 2.5 hours, showing (a) T-shape and (b) L-shape. (c) SEM image and elemental mapping of an area with a Ga_2O_3 nanowire and a SnO_2 nanobelt marked by arrow. The inset displays a magnified area of the SnO_2 nanobelt revealing the jagged edges.

with other dimensionalities, such as nanoparticles or flakes, by thermal methods has been scarcely explored.

In this work, the formation of SnO_2 nanostructures with different dimensionalities in a single step process, in which Ga_2O_3 nanowires act as scaffold or catalyst, has been investigated. Metallic Ga and SnO_2 powders have been used as initial source materials and Ga_2O_3 pellets as substrates. Samples obtained after 2.5, 8.0 and 15.0 hours of thermal treatment at 1500 ºC have been characterized by electron microscopy related techniques. It has been found that tin oxide is self-organized segregated over the Ga_2O_3 nanowires, leading to the formation of SnO_2 particles on a 3D-growth basis for short treatments. However, 2D-growth of SnO_2 flakes, attached to Ga_2O_3 nanowires or isolated, was observed for longer treatments. The results in this article would contribute to the understanding on the growth mechanisms of complex nanostructures of oxides with several dimensionalities. These architectures could be good candidates to upgrade the functionalities of energy and sensor devices where tin oxide plays an active role.

Experimental

A catalyst-free evaporation deposition method has been used to grow the SnO_2/Ga_2O_3 oxide nanostructures. Metallic gallium bits and tin oxide powders placed on the top of a gallium oxide pellet acting as substrate have been thermally annealed at 1500 ºC in an open furnace under an argon flux of 0.8 l/min. The melting point of Ga_2O_3 is 1725 ºC while of SnO_2 is 1630 ºC, thus the thermal treatment at 1500 ºC lies in the window temperature to nucleate nanostructures of both oxides under conditions of a supersaturated atmosphere. Several runs, for 2.5, 8.0 and 15.0 hours, have been conducted to study the evolution of the formed nanostructures starting with the same precursor materials. After annealing, a high amount of white nanostructured wool-like material is observed on the substrate pellet. The nanostructures are then transferred to either a silicon substrate or a copper grid for characterization by scanning electron microscopy (SEM) and (scanning) transmission electron microscopy (S/TEM) techniques. The equipment used was a Leica Steroscan SEM for Energy Dispersive X-ray spectroscopy (EDS) measurements. A JEOL 2100 TEM and a double-corrected JEOL ARM 200F were used for a high-resolution structural and chemical characterization of the nanostructures.

Results and discussion

Ga_2O_3 pellet was fully covered with nanostructures after 2.5 hours of thermal treatment, which were transferred out to a silicon substrate for SEM characterization. The most common were branched Ga_2O_3 wires (~ 1 µm width and tens of microns in length) leading to T or L shapes structures, with SnO_2 preferentially covering one of the branches. Figure 1 corresponds to secondary electron SEM images of T and L nanostructures (Figures 1(a) and (b) respectively) and the associated Ga and Sn elemental mapping, which reveals that Sn decorates the Ga_2O_3 branches in a selective way. Occasional SnO_2 nanobelts were also found, as the one indicated by an arrow in Figure 1(c). This image shows a SnO_2 nanobelt located next to a Ga_2O_3 nanowire. Surface differences between them are noticeable; whereas Ga_2O_3 nanowire exhibits smooth surface, SnO_2 belt has jagged edges, clearly observed in the inset corresponding to a magnified image of the area inside the green rectangle in figure 1(c). The results indicate that Ga_2O_3 nanowires are produced in an efficient manner, after 2.5 hours of thermal treatment and supersaturated oxygen atmosphere conditions. The presence of SnO_2 among the precursors promotes the formation of branched Ga_2O_3 nanowires, as we previously reported[13]. Here, we have increased the SnO_2 amount and as a result, a SnO_2 shell around one of the Ga_2O_3 branches has been formed.

Longer thermal treatments (8 hours) were carried out to analyze the evolution of these morphologies. Figure 2(a) shows a secondary electron image of the pellet annealed 8 hours, in which some nanowires present fuzzy lateral walls. Figures 2(b) and 2(c) display TEM images of some of these structures. As it can be seen, the nanowires appear decorated with diamond-like particles and/or with ultrathin belts or flakes. Hence, the increase of the duration of the thermal treatment and the presence of SnO_2 during the growth process seems to promote both the nucleation of SnO_2 crystallites and the formation of SnO_2 belts on Ga_2O_3 nanowires.

View Article Online
DOI: 10.1039/C7CE01311F
Crystal Engineering Communications ARTICLE

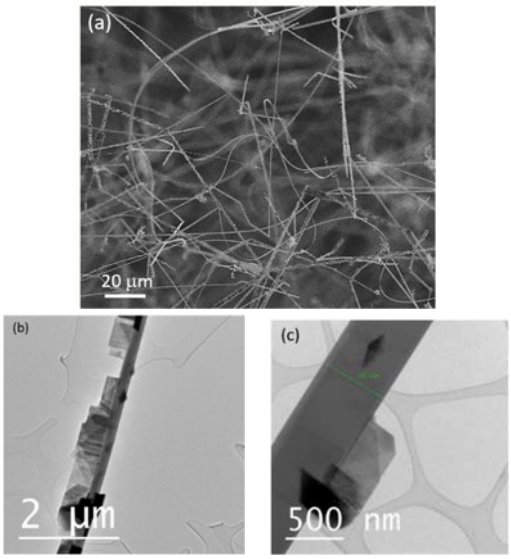

Fig. 2 (a) SEM image of the pellet after 8 hours of treatment. (b-c) TEM images of thinner Ga_2O_3 nanowires decorated with well-faceted particles and thin flakes.

In order to get a more microscopic view of these nanostructures, STEM and EDS mappings were perfomed. Figure 3(a) corresponds to an ADF-STEM image of a Ga_2O_3 wire decorated with diamond-shaped particles. EDX elemental distribution carried out in the magnified area enclosed in the red rectangle confirmed the diamond-shaped particles are made of SnO_2. The SnO_2 diamonds have the same orientation and they are arranged with the diagonal directions parallel and perpendicular to the main Ga_2O_3 axis microwire. SAED pattern carried out in one of these wires reveals the [001] direction as the Ga_2O_3 axis (Figures 3(b)-(c)). The overlapping of some spots of the SnO_2 and Ga_2O_3 indicates a partial lattice matching, (111) Ga_2O_3 with (-101) SnO_2 planes, between both structures in this orientation However, the promotion of the 3D growth of SnO_2 particles over the Ga_2O_3 wire was observed instead of a layer-by-layer epitaxial growth.

In addition, thermal treatment for 8 hours also produces some thinner Ga_2O_3 nanowires (of about 200 nm wide) holding SnO_2 flakes and eventually SnO_2 particles. Figure 4(a) corresponds to a bright field STEM image of a 200 nm width Ga_2O_3 nanowire decorated with SnO_2 nanofins, as the elemental mapping demonstrates. A Sn-rich overlayer at the Ga_2O_3 nanowire surface was also revealed in these nanostructures, as it can be observed in the elemental maps of figure 4(a) and (b), along with a Sn-rich thin stripe running along the middle of the main NW axis (Figure 4(b)). It is well known that dopant impurities end to out-diffuse to the surface or accumulate at planar defects. High-resolution ADF-STEM image of the dashed square marked in Figure 4(b) indicates that Sn atoms accumulate along a twin in the Ga_2O_3 along the NW axis. The Sn at the twin boundary originates some local structural change as figure 4(c) suggests. It has

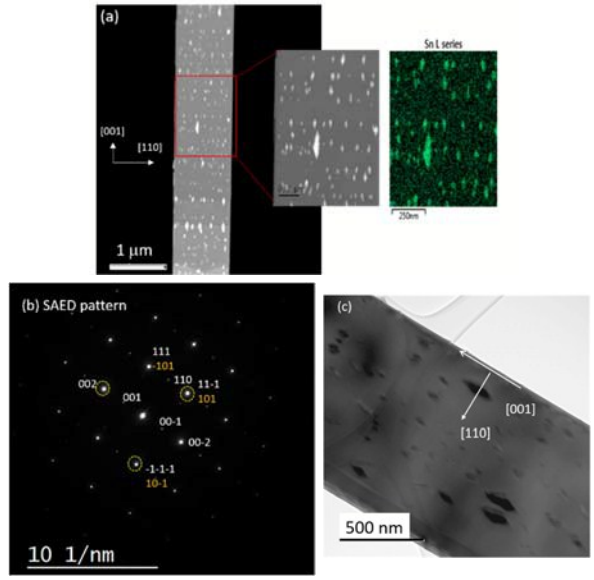

Fig. 3 (a) ADF-STEM image of a Ga_2O_3 nanowire and EDS mapping of Sn element. The microanalysis reveals that the tiny diamond-shaped particles are SnO_2. (b) SAED pattern of the decorated nanowire. Diffraction spots have been indexed according to the Ga_2O_3 [-110] zone axis (white labels) and the SnO_2 zone axis [010] (orange labels) . (c) Bright field TEM image taken with less intense diffraction spot.

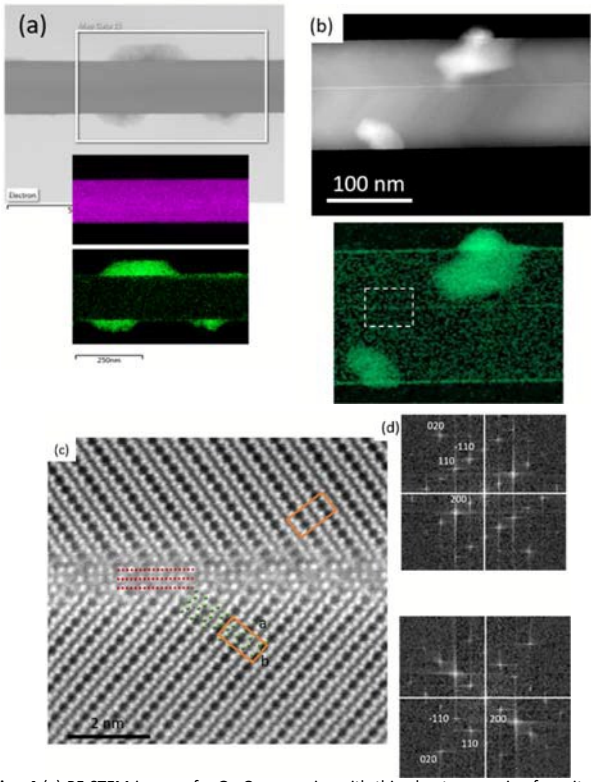

Fig. 4 (a) BF-STEM image of a Ga_2O_3 nanowire with thin sheets emerging from its surface. Lower image: EDS mapping of Ga and Sn elements, in pink and green, respectively. (b) ADF-STEM image and EDS Sn mapping of a twinned Ga_2O_3 nanowire, which shows that Sn accumulates at the surface and at the twin plane. (c) Atomic resolution ADF-STEM image taken from the area enclosed the square highlighted in (b). (d) FFT corresponding to the upper and lower parts of the image indexed according to Ga_2O_3 [001] zone axis.

View Article Online
DOI: 10.1039/C7CE01311F

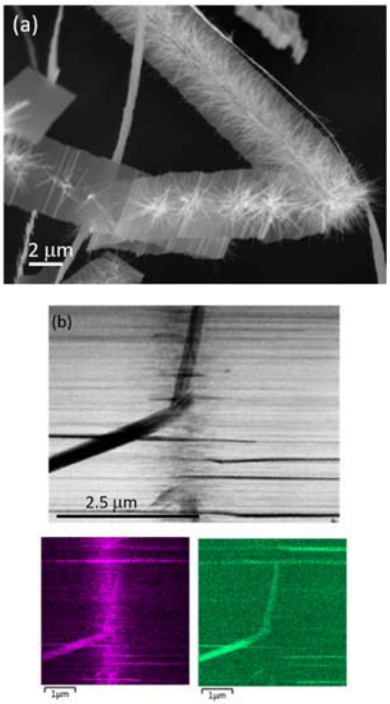

Fig. 5 (a) SEM image of a SnO_2 belt with emergent nanowires obtained after 15 hours. (b) STEM image and (c) EDS mappings of Ga (pink) and Sn (green) elements of the central part of one of the SnO_2. belts.

been reported that β-Ga_2O_3 structure reacts with MO_2 oxides with the rutile structure and ternary $Ga_4M_{n-4}O_{2n-2}$ compounds have been stabilized, where M could be Ge, Ti or Sn[19]. The three plane layers resolved at the NW axis (indicated with red lines in the figure) could agree with the initial formation stage of a ternary compound. Fourier transforms were carried out in top and bottom areas of the twin boundary (figure 2(d)), agreeing with the [001] Ga_2O_3 projection. The formation of the Sn-rich overlayer at the NW surface seems to promote the 2D-growth of SnO_2 on gallium oxide nanowires for samples treated for 8 hours, as Figure 4(b) shows.

These results show that tin oxide nucleates at specific sites of the Ga_2O_3 nanowires, leading to non-conventional heterostructures with dissimilar dimensionality, in which Ga_2O_3 nanowires act as substrate. By increasing the duration of the thermal treatment up to 15 hours, high population of SnO_2 belts are formed, some of which are bicrystals. Figure 5(a) shows a SEM image of a SnO_2 belt with a central axis from which nanowires emerge. Figure 5(b) shows the STEM image and its corresponding EDS mapping of one of these belts that reveal accumulation of Ga atoms along the central axis. Quantitative data at the central area give Sn, Ga and O concentrations of 18 %, 18 % and 63 % atomic percentage, respectively, whereas the atomic proportion near the belt edge is [Sn] = 31,2 %, [Ga] = 6,3 % and [O] = 62,5%.

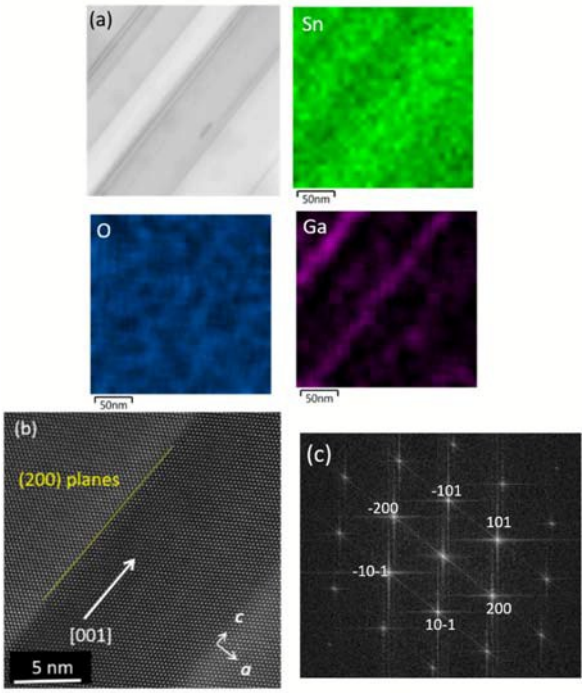

Fig. 6 (a) EDS-STEM mapping of a SnO_2 belt. (b) Annular dark field (ADF) image at higher magnification. (c) FT of the ADF image. Spots are indexed according the [010] zone axis of SnO_2.

High magnification EDS compositional mapping revealed Ga accumulation in the SnO_2 belts along a preferential direction (Figure 6). Figure 6(a) corresponds to an area of the SnO_2 belts with parallel contrast perpendicular to the main axis. Elemental Sn, O and Ga maps demonstrate the inhomogeneity of the belts, with areas with higher Ga content in their structure. A high magnification annular dark field (ADF) STEM image is displayed in Figure 6(b). The FFT of the area is indexed according to the [010] zone axis of rutile SnO_2 structure (Figure 6(c)). The direction and planes of the parallel fringes are identified as [001] direction in (200) planes. These planes seem to be preferential sites for Ga gathering in the SnO_2 structure. Although the FT symmetry agrees with the SnO_2 rutile, the spots distances are slightly shortened (around 1 %) in comparison with those corresponding to the perfect rutile SnO_2 lattice structures, implying a strained or modified lattice. In particular, the presence of SnO layers, with slightly larger lattice parameters than SnO_2 rutile phase or sub-stoichoimetric oxides SnO_{2-x}, cannot be ruled out. SnO oxide is a layered oxide that usually ends up in SnO_2 as stable phase. There are several works that report the synthesis of stannous oxide in the form of flakes, which are rather easily produced due to the van der Waals bonding within the unit cell[10,20-21]. In addition, it has been suggested that SnO could serve as template to create complex SnO_2 nanostructures[22,23]. Actually, one of the ways to synthetize SnO is from reduction of SnO_2[24]. Theoretically, the structural transformation of SnO_2 into SnO can be easily explained through a rotation along [010] axis and removal of a row of oxygens of the (200) plane[25]. Since tin oxide has oxygen vacancies, some kind of SnO_{2-x} compound is expected

View Article Online
DOI: 10.1039/C7CE01311F
Crystal Engineering Communications ARTICLE

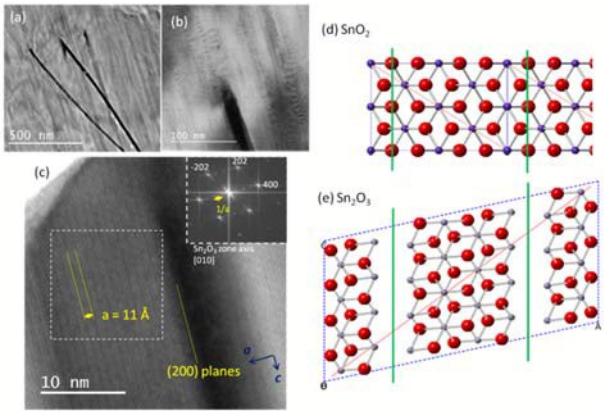

Fig. 7 (a) Low magnification TEM of a SnO_2 belt with emergent nanowires. (b) Detail of the junction area and moiré fringes. (c) High resolution image of the belt. Inset: SAED pattern indexed with the SnO_2 rutile structure. Crystalline structure of (d) SnO_2 and (e) Sn_2O_3. Both are viewed from the [010] direction. When oxygen vacancies are ordered along green line, (parallel to (200) planes) the lattice easily converts into Sn_2O_3 with a slight distortion of Sn-O bonds.

and it could be possible that ordering of O vacancies leads to a local microstructural change. In our case, we have used SnO_2 as starting material along with metallic gallium. On the other hand, it should be mentioned that if no gallium is in the precursors, no SnO_2 belts are formed. Therefore, it seems that gallium atoms act as a catalyst for the formation of these ultrathin belts.

A structure composed of GeS nanosheets (2D) emerging from GeS nanowires (1D) has been recently reported[26]. One of the key requirements to achieve these mixed dimensional heterostructures is the need of a layered graphite-like material. The growth occurred in two steps, the GeS nanowires were firstly formed and a controlled oxidation of the surface led to the formation of GeS nanosheets in a second step[26]. Here, we observe that SnO_2 belts, as those of figure 2(b), are formed during a long thermal treatment in a one-step process. In addition, we have also found that a significant Ga accumulation takes place at the central part of the SnO_2 belts. As observed in Figure 5(a), nanowires emerge from the central area of SnO_2 belts. Figure 7(a) corresponds to a TEM image of one belt with nanowires coming out from it. A magnified image of the junction area reveals moiré fringes in the SnO_2 layer (Figure 7(b)). A high-resolution image is shown in Figure 7(c) along with the FT pattern from the dashed square. It is clearly observed an extra periodicity of 11 Å along [100] direction and, consequently, extra spots arise in the FT pattern (see inset). These results suggest ordering in defects allocation that could lead to a supercell structure. It is well known that oxygen vacancies are common in oxide materials. Seko *et al.* [25] propose that the alignment of oxygen vacancies along (101) planes in SnO_2 leads to structures composed of SnO_2-like and SnO-like local structures that could be compatible with the oxygen deficiency, e.g. SnO_{2-x}. They propose a series of homologous structures of tin oxides, Sn_3O_4 (x= 4/3, closer to SnO) and Sn_2O_3 (x= 3/2, closer to SnO_2) as intermediate oxides, in which Sn exhibits mixed valence states. However, there was not still experimental confirmation of this suggestion.

Figures 7(d) and 7(e) show the crystalline structure of SnO_2 and Sn_2O_3 view from the [010] direction. Green lines are highlighting oxygen planes parallel to (200) planes in the rutile structure. When oxygen ions are removed from these green lines, the lattice easily converts into an intermediate oxide (Sn_2O_3) with a slight distortion of Sn-O bonds[25]. Sn_2O_3 is a metastable phase in which oxidation states of Sn are mixed (both Sn^{2+} and Sn^{4+}) to counterbalance the electronic charge. On the other hand, these quasi-empty oxygen (200) planes would provide room to accommodate Ga^{3+} ions into the SnO_2 crystal. This is consistent with our observations by STEM-EDS analysis, in which Ga impurities concentration is higher at these preferred planes, i.e. gallium impurities are gathered at defected planes in SnO_2 lattice. Actually, our TEM results could well agree with the presence of a local intermediate oxide (Sn_2O_3) phase as it can be seen in Figure 7. Lattice parameters of Sn_2O_3 are a = 11.1 Å, b = 4.89 Å and c = 5.84 Å, and β = 77.1°. The HRTEM image (Figure 7b) shows the lattice spacing a of 11 Å. The reduced FT pattern from the dashed area displays extra spots that can be indexed as (100) (200) (300) planes of this structure accordingly. Most of the applications of tin oxide nanomaterials (transparent conductive oxide and solid-state gas sensor) relies on their surface properties[27] and in particular on the oxygen stoichiometry. In this work, we have obtained Ga doped SnO_2 belts that exhibit the (010) surface. The results show that the incorporation of Ga atoms is linked to changes in the oxygen vacancies population. This could affect the performance of doped tin oxide plates in electrodes or gas sensor devices.

Conclusions

A high amount of complex nanostructures involving Ga_2O_3 and SnO_2 nanomaterials have been achieved by a simple evaporation method. In this work, we report the 3D and 2D growth of SnO_2 nanostructures on Ga_2O_3 nanowires. The source materials were metallic gallium and tin oxide powders on the top of a compacted gallium oxide pellet acting as substrate. The synthesis route is catalyst-free and the process is self-catalyzed. Thermal growth treatments for 2.5, 8.0 and 15.0 hours, were conducted in three separated runs. The process leads to the formation of tin-doped gallium oxide nanowires as the first step. Sn impurities inside the gallium oxide lattice are diffused towards the surface or gathered in defective planes. The accumulation of Sn atoms promotes the nucleation of tin oxide nanostructures in a different manner depending on the duration of thermal treatment. 3D-growth of tin oxide nanoparticles and 2D-growth of thin flakes on Ga_2O_3 nanowires have been found for shorter thermal treatments. On the other hand, 2D-growth of Ga-doped SnO_2 belts and flakes have also been produced after the longer treatments. TEM results show that Ga impurities lie on (200) SnO_2 planes and could stabilize

View Article Online
DOI: 10.1039/C7CE01311F

some non-stoichiometric tin oxides (SnO_{2-x}). The results support that the growth parameters and the suitable combination of two oxide materials enable somehow shape engineering that produce 3D, 2D and 1D nanomaterials.

Acknowledgements

This work has been supported by MINECO (projects CSD 2009-2013, MAT 2012-31959, MAT 2015-65274-R-FEDER). We thank Richard Beanland for his advice at Warwick University. M. A-O acknowledges financial support from MEC (FPU contract). B.M acknowledges the mobility Grant supported by MEC (PRX14/00134) for sabbatical leave at Warwick University.

References

1 A. Kolmakov, D. Klenov and Y. Lilach, *Nano Lett.*, 2005, **5**, 667-673.
2 E. Comini, G. Faglia, G. Sberveglieri, Z. Pan and Z. L. Wang, *Appl. Phys. Lett.*, 2002, **81**, 1869-1871.
3 I. López, A. Castaldini, A. Cavallini, E. Nogales, B. Méndez and J. Piqueras, *J. Phys. D: Appl. Phys.*, 2014, **47**, 415101.
4 C. Cheng, B. Liu, H. Yang, W. Zhou, L. Sun, R. Chen, S. F. Yu, J. Zhang, H. Gong, H. Sun and H. J. Fan*, ACS Nano.*, 2009, **3**, 3069-3076.
5 C. Cheng and H. J. Fan, *Nano Today.*, 2012, **7**, 327-343.
6 E. P. Stuckert, R. H. Geiss, C. J. Miller, and E. R. Fisher, *ACS Appl. Mater. Interfaces* 2016, **8**, 22345−22353.
7 O. Lupan, L. Chow, G. Chai, H. Heinrich, S. Park and A. Schulte, *J. Cryst. Growth*, 2008, **311**, 152−155.
8 D. Cai, T. Yang, D. Wang, X. Duan, B. Liu, L. Wang, Y. Liu, Q. Li and T. Wang, *Electrochimica Acta*, **159**, 2015, 46–51.
9 J. Mei, T. Liao, L. Kou and Z. Sun, *Adv. Mater.* 2017, **6,** 1700176.
10 Y. Cui, F. Wang, M. Z. Iqbal, Y. Li, A. M. Toufiq, Z. Wang, Z. Wang and S. Ali, *Crys. Res. Technol.*, 2015, **50**, 210-214.
11 D. Wang, F. Qian, C. Yang, Z. Zhong and C. M. Lieber, *Nano Lett.*, 2004, **4**, 871-874.
12 J. G. Wen, J. Y. Lao, D. Z. Wang, T. M. Kyaw, Y. L. Foo and Z. F. Ren, *Chem. Phys. Lett.*, 2003, **372**, 717-722.
13 I. López, E. Nogales, B. Méndez, J. Piqueras, A. Peche, J. Ramirez-Castellanos and J. González-Calbet, *J. Phys. Chem C*, 2013, **117**, 3036-3045.
14 G. Martínez-Criado, J. Segura-Ruiz, M. H. Chu, R. Tucoulou, I. López, B. Méndez and J. Piqueras, *Nano Lett.*, 2014, **14**, 5479-5487.
15 M. García-Tecedor, D. Maestre, A. Cremades and J. Piqueras, *J. Mat. Chem. C.*, 2016, **4**, 5079.
16 I. López, A. Utrilla, E. Nogales, B. Méndez, J. Piqueras, A. Peche, J. Ramírez-Castellanos and J. González-Calbet, *J. Phys. Chem. C.*, 2012, **116**, 3935-3943.
17 M. García-Tecedor, D. Maestre, A. Cremades and J. Piqueras, *J. Phys. Chem. C.*, 2016, **120**, 22028-22034.
18 M. Alonso-Orts, A. M. Sánchez, S. A. Hindmarsh, I. López, E. Nogales, B. Méndez and J. Piqueras, *Nano Lett.*, 2017, **17**, 515-522.
19 D. D. Edwards, T. O. Mason, W. Sinkler, L. D. Marks, K. R. Poeppelmeier, Z. Hu and J. D. Jorgensen, *J. Solid State Chem.,* 2000, **150**, 294-304.
20 B. Liu, J. Ma, H. Zhao, Y. Chen and H. Yang, *Appl. Phys. A*, 2012, **107**, 437-443.
21 Z. L. Wang and Z. Pan, *Adv. Mater.*, 2002, **14**, 1029-1032.
22 H. Wang, Y. Wang, J. Xu, H. Yang, C. S. Lee and A. L. Rogach, *Langmuir*, 2012, **28**, 10597-10601.
23 K. M. Li, Y. J. Li, M. Y. Lu, C. I. Kuo and L. J. Chen, *Adv. Funct. Mater.*, 2009, **19**, 2453-2456.
24 Z. R. Dai, Z. W. Pan and Z. L. Wang, *J Am. Chem. Soc.*, 2002, **124**, 8673-8680.
25 A. Seko, A. Togo, F. Oba and I. Tanaka, *Phys. Rev. Lett., 2008,* **100**, 045702.
26 C. Li, Y. Yu, M. Chi and C. Cao, *Nano Lett.*, 2013, **13**, 948-953.
27 M. Batzill and U. Diebold, *Prog. Surf. Sci. 2005,* **79,** 47-154.